Supplementary Table 1 Cryo-EM Data Collection, Refinement, and Validation Statistics

Data Collection and Processing	**D2-GoA^{K46E}**	**DRD2-GoA^{K46E}-scFv16**
EMDB Accession Number		
PDB Accession Number		
Voltage (kV)	200	200
Electron exposure (e-/Å2)	55.0	55.0
Number of movies	3161	3827
Defocus range (μm)	-0.1 to -2.8	-0.1 to -2.8
Defocus Mean (SD) μm [1]	1.1(0.4)	1.4(0.4)
Physical Pixel Size (Å)	0.88	0.88
Particles for 3D classification	296,893	332,959
Particles for final map	153,270	216,188
Map Resolution (Å) [2]	3.28	3.20
Symmetry Imposed	C1	C1
FSC Threshold	0.143	0.143
Refinement		
Initial Model Used (GPCR/G protein)	8IRS/1GP2	8IRS/1GP2
Model composition		
Non-hydrogen atoms	8001	8799
Protein residues	1015	1123
Ligands	1	1
Lipids	0	0
Mean B-factors (Å^2)		
Protein	102.6	82.8
Ligand	20.0	66.6
RMSD		
Bond length (Å)	0.004	0.003
Bond angle (°)	0.881	0.682
Validation		
MolProbity score	1.39	1.53
Clash score	5.69	9.29
Poor rotamer (%)	0.23	0.31
Ramachandran Plot		
Favored (%)	97.6	97.8
Allowed (%)	2.4	2.2
Disallowed (%)	0.00	0.00

[1] Underfocus
[2] Resolution estimates from cryoSPARC auto-corrected GSFSC
NA – Not Applicable

Supplementary Table 2 | D1R/D2R Orthosteric Contact Summary List

BW*	D2R/GoA (KE)	D2R/GoA (KE)/scFv16	D2R/Rotigotine (PDB ID 8IRS)	D1R/Dopamine (PDB ID 7F1O)
2.61			V91	
2.64			L94	
3.32	D114	D114	D114	D103
3.33	V115	V115	V115	I104
3.36	C118	C118	C118	S107
3.37	T119	T119	T119	T108
ECL2			I183	
ECL2	I184		I184	L190
5.38	F189	F189		Y194
5.39				
5.42	S193	S193	S193	S198
5.43				
5.46	S197	S197	S197	S202
6.48	W386	W386	W386	W285
6.51	F389	F389	F389	F288
6.52	F390	F390	F390	F289
6.55	H393	H393	H393	N292
7.35			Y408	
7.39	T412	T412	T412	V317
7.43	Y416	Y416	Y416	W321

*Ballesteros-Weinstein Designation

Supplementary Table 3 | D2R to GoA^{K46E} Contact Summary List

CGN	D2/GoA (KE)	D2R	BW
S1.2	V34	M140*	ICL2
S3.1	L195	M140*	ICL2
N/A	N316	K367	6.29
H5.13	D341	R219*	5.68
		V223	5.72
H5.15	I343	P139*	ICL2
		M140*	ICL2
		N143*	ICL2
H5.16	I344	V136*	3.54
		P139*	ICL2
		R219	5.68
H5.19	N347	A135*	3.53
		P139*	ICL2
		Y142*	ICL2
		N143*	ICL2
H5.20	L348	V136*	3.54
		L216*	5.65
H5.21	R349	K367	6.29
H5.23	C351	T69*	2.39
		R132*	3.50
		A135*	3.53
		Y142*	ICL2
H5.25	L353	R132*	3.50
		A371*	6.33
		M374*	6.36
		L375*	6.37
H5.26	Y354	L216*	5.65
		K367	6.29
		E368*	6.30
		A371*	6.33

Note – BW:Ballesteros-Weinstein Designation; CGN: Common Gα Numbering (CGN) scheme; (*) indicates shared D2R interaction between GoA^{K46E} and G_{i1} .N/A – no CGN numbering for this region.

Supplementary Table 4 | D2R to Gi1 (PDB 8IRS) Contact Summary List

CGN	D2R/Gi1	D2	BW
HN.48	R24	Y146	4.36
N/A	A31	T144	4.34
S3.1	L194	M140*	ICL2
N/A	E318	E368*	6.30
H5.11	V339	M140*	ICL2
H5.12	T340	P139*	ICL2
H5.13	D341	R219*	5.68
H5.15	I343	P139*	ICL2
		M140*	ICL2
		N143*	ICL2
H5.16	I344	P139*	ICL2
		L216*	5.65
		R219*	5.68
H5.17	K345	R219*	5.68
		E368*	6.30
H5.19	N347	A135*	3.53
		P139*	ICL2
		Y142*	ICL2
		N143*	ICL2
H5.20	L348	V136*	3.54
		L216*	5.65
		R219*	5.68
H5.22	D350	T67	2.37
		Y142*	ICL2
H5.23	C351	T69*	2.39
		R132*	3.50
		A135*	3.53
		Y142*	ICL2
H5.25	L353	R132*	3.50
		V136*	3.54
		I212	5.61
		L216*	5.65
		A371*	6.33
		M374*	6.36
		L375*	6.37
H5.26	F354	R219*	5.68
		E368*	6.30
		K370	6.32
		A371*	6.33

Note – BW:Ballesteros-Weinstein Designation; CGN: Common Gα Numbering (CGN) scheme; (*) indicates shared D2R interaction between GoA^{K46E} and G_{i1} .N/A – no CGN numbering for this region.

Supplementary Table 5 | Mutagenesis Primers

Oligo Name	Oligo Sequence (5' - 3')
Ga13_K61E_fwd	GCGGCGAATCCACCTTCCTGAAGCAGATGCG
Ga13_K61E_rev	GTGGATTCGCCGCTCTCGCCCGC
Ga13_R230C_fwd	CAGAATGTAAACGTTGGTTTGAATGTTTCGACAGTG
Ga13_R230C_rev	CGTTTACATTCTGATCTCTGACCACCTACATCAACC
Ga15/16_K55E_fwd	GCGGGGAAAGCACCTTCATCAAGCAGATGCG
Ga15/16_K55E_rev	GTGCTTTCCCCGCTCTCGCCTGGG
Ga15/16_R216C_fwd	CAGAGTGTAAGAAATGGATCCATTGTTTCGAGAACGTG
Ga15/16_R216C_rev	TTCTTACACTCTGACTTCTGGCCCCCGAC
Gai2_K46E_fwd	CAGGGGAAAGCACCATCGTCAAGCAGATGAAG
Gai2_K46E_rev	GTGCTTTCCCCTGACTCCCCAGCACCC
Gai2_R209C_fwd	CTGAGTGTAAGAAGTGGATCCACTGCTTTGAGGG
Gai2_R209C_rev	TTCTTACACTCAGACCGCTGACCACCC
Gai3_K46E_fwd	CTGGTGAAAGCACCATTGTGAAACAGATGAAAATCATTCATG
Gai3_K46E_rev	GTGCTTTCACCAGATTCTCCAGCACCGAGTAG
Gai3_R208C_fwd	CAGAATGTAAAAAGTGGATTCACTGTTTTGAGGGAGTG
Gai3_R208C_rev	TTTTTACATTCTGATCTTTGGCCACCTACATCAAACATC
Gaq_K52E_fwd	GTGGCGAAAGTACGTTTATCAAGCAGATGAGAATCATCCATG
Gaq_K52E_rev	GTACTTTCGCCACTCTCTCCTGTCCCGAG
Gaq_R213C_fwd	CAGAGTGTAGAAAATGGATACACTGCTTTGAAAATGTCACC
Gaq_R213C_rev	TTTCTACACTCTGACCTTTGGCCCCCTACATC
Gas_K53E_fwd	CTGGTGAAAGCACCATTGTGAAGCAGATGAGG
Gas_K53E_rev	GTGCTTTCACCAGATTCTCCAGCACCCAGC
Gas_R231C_fwd	ATGAATGTCGCAAGTGGATCCAGTGCTTCAAC
Gas_R231C_rev	TTGCGACATTCATCGCGCTGGCCACC
Gaz_K46E_fwd	CAGGCGAAAGCACCATCGTCAAACAGATGAAGATC
Gaz_K46E_rev	GTGCTTTCGCCTGAGTTGCTGGTGCCC
Gaz_R209C_fwd	CAGAGTGTAAAAAGTGGATCCACTGCTTCGAGG
Gaz_R209C_rev	TTTTTACACTCTGACCTCTGCCCCCCC
Ga11_K52E_fwd	GCGGGGAAAGCACGTTCATCAAGCAGATGCG
Ga11_K52E_rev	GTGCTTTCCCCGCTCTCGCCCGTG
Ga11_R213C_fwd	CGGAGTGTAGGAAGTGGATCCACTGCTTTGAGAAC
Ga11_R213C_rev	TTCCTACACTCCGACCGCTGGCCC
Gai1_K46E_fwd	CTGGTGAAAGTACAATTGTGAAGCAGATGAAAATTATCCATGAAG
Gai1_K46E_rev	GTACTTTCACCAGATTCACCAGCACCGAG
Gai1_R208C_fwd	CTGAGTGTAAGAAGTGGATTCATTGCTTCGAAGGAG
Gai1_R208C_rev	TTCTTACACTCAGATCTCTGACCTCCCACATCAAAC
Gao_K46E_rev	GTGCTTTCTCCTGATTCTCCAGCCCCGAG
Gao_K46E_fwd	CAGGAGAAAGCACCATTGTGAAGCAG
Gao_R209C_fwd	CTGAATGTAAGAAGTGGATCCATTGCTTCGAGGAC
Gao_R209C_rev	TTCTTACATTCAGATCGCTGGCCTCCGACGTCAAAC

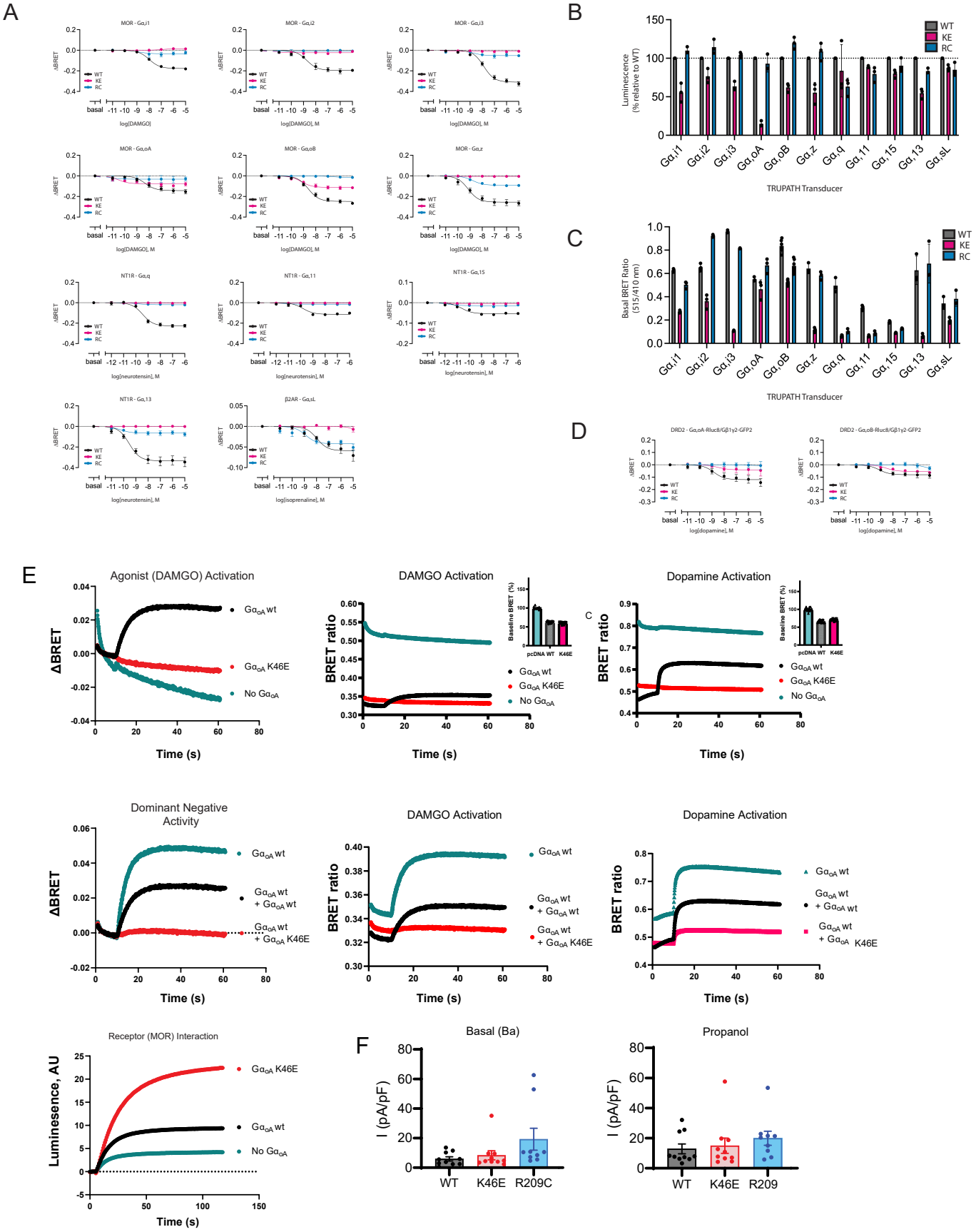
A
MOR - Gαi1
MOR - Gαi2
MOR - Gαi3
MOR - GαoA
MOR - GαoB
MOR - Gαz
NT1R - Gαq
NT1R - Gα11
NT1R - Gα15
NT1R - Gα13
β2AR - GαsL
ΔBRET
WT
KE
RC
basal
log[DAMGO], M
log[neurotensin], M
log[isoprenaline], M
B
Luminescence (% relative to WT)
Gαi1
Gαi2
Gαi3
GαoA
GαoB
Gαz
Gαq
Gα11
Gα15
Gα13
GαsL
TRUPATH Transducer
C
Basal BRET Ratio (515/410 nm)
D
DRD2 - GαoA-Rluc8/Gβ1γ2-GFP2
DRD2 - GαoB-Rluc8/Gβ1γ2-GFP2
log[dopamine], M
E
Agonist (DAMGO) Activation
ΔBRET
GαoA wt
GαoA K46E
No GαoA
Time (s)
DAMGO Activation
BRET ratio
Baseline BRET (%)
pcDNA WT
K46E
Dopamine Activation
Dominant Negative Activity
GαoA wt + GαoA wt
GαoA wt + GαoA K46E
Receptor (MOR) Interaction
Luminesence, AU
F
Basal (Ba)
I (pA/pF)
WT
K46E
R209C
Propanol
R209

Supplementary Figure 1. pinKE mutations impede Gβγ dissociation.

(A) HEK293 cells transfected with the indicated receptor, the indicated subtype of WT or mutant Gα-RLuc8 donor, Gβ and Gγ-GFP acceptor proteins. Representative DAMGO, neurotensin, and isoprenaline concentration-response curves measuring G protein dissociation (ΔBRET) using the μ-opioid (G_{i1}, G_{i2}, G_{i3}, G_{i3}, G_{oA}, G_{oB}, G_z), neurotensin (G_q, G_{11}, G_{13}, G_{15}), or β_2-adrenergic receptor (G_s).
(B) Expression levels of pinKE (pink) and triadRC (blue) Gα-Rluc8 subunits normalized relative to wildtype (gray), determined using luminescence values from HEK293 cells transfected with each indicated construct. Data are means ± SEM from 3 independent experiments, each performed with 2 replicates.
(C) Representative dopamine concentration-response curves measuring G protein dissociation (ΔBRET) using the dopamine D_2 receptor (G_{oA}, G_{oB}) paired with the subunits ($G\beta_1$ and $G\gamma_2$) used for cryo-EM structure determination. Data are means ± SEM from 3 independent experiments, each performed with 2 replicates.
(D) Association of pinKE (pink) and triadRC (blue) Gα-Rluc8 subunits with Gβ and Gγ-GFP2 relative to wildtype (gray), determined by calculating the basal BRET ratio (515/410 nm) from HEK293 cells transfected with each indicated construct and treated with vehicle.
(E) HEK293 cells transfected with μ opioid receptor (MOR) after agonist (DAMGO), wildtype or mutant $G\alpha_o$, masGRK3ct-Nluc-HA donor and Venus-Gβγ acceptor proteins. Representative time-course measurements after agonist (DAMGO) addition presented as ΔBRET (top). Also shown are the raw BRET values after agonist (DAMGO or dopamine) addition, presented as BRET ratio. Inset, BRET ratios before agonist addition, presented as a baseline percentage of vector control (pcDNA).
(F) Bar plot of current recordings from HEK293T transfected with the μ opioid receptor (MOR) and wildtype or mutant $G\alpha_o$, after treatment with barium (Ba^{2+}) or propanol. Data are means ± SD from 9 (R209C) or 10 (WT, K46E) independent experiments.

A

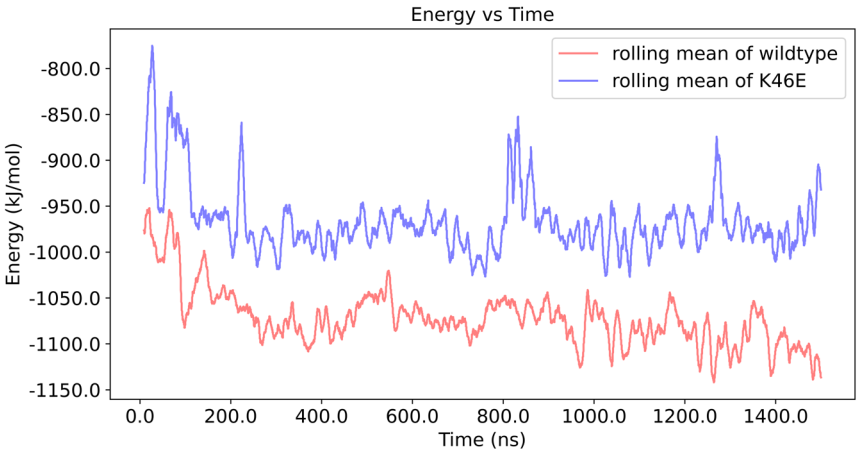

B

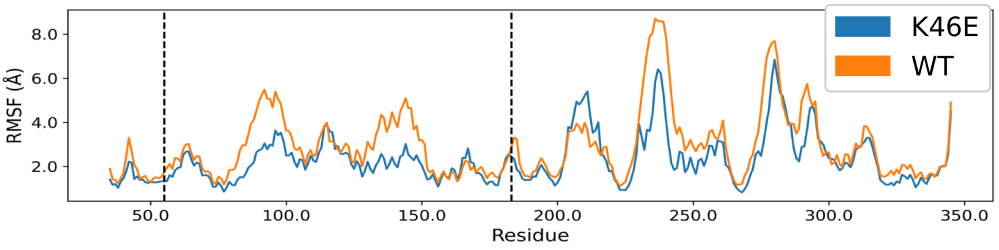

C

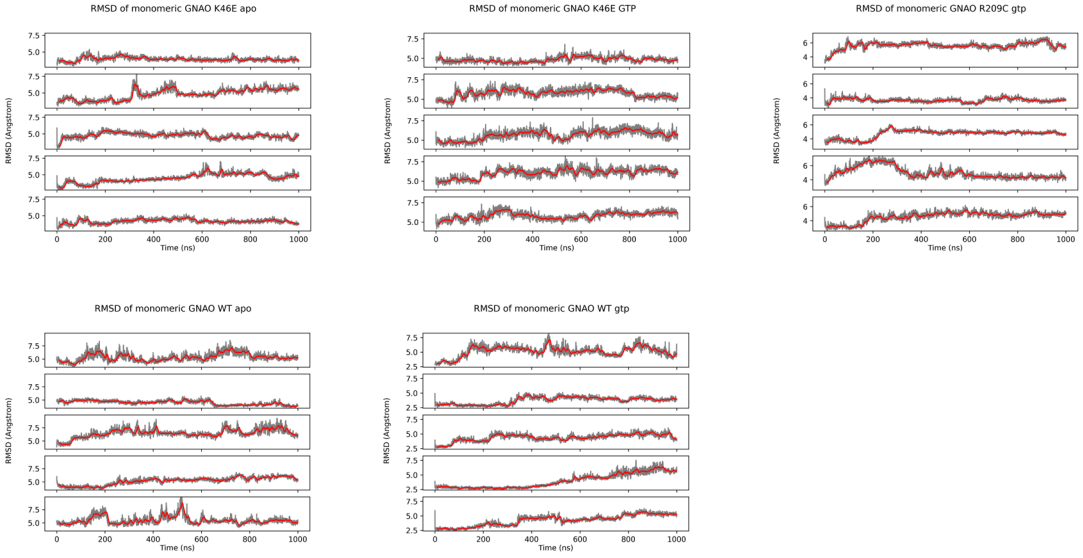

Supplementary Figure 2. Contact frequency of residues in the GTP binding site.

(A) Residues that show at least 30% decrease in frequency of contacts with GTP in the $G\alpha_o^{K46E}$-GTP system compared to those with GTP in the WT $G\alpha_o$-GTP system during simulations. Locations of the residues are approximate.
(B) Quantitative RMSF plot showing that the flexibility of the wildtype residues (as reflected by RMSF) are higher than those in the K46E mutant (for all but residues 206-216).
(C) C-alpha RMSD plot of each frame in a trajectory against the starting structure. Unit is in angstroms.

A

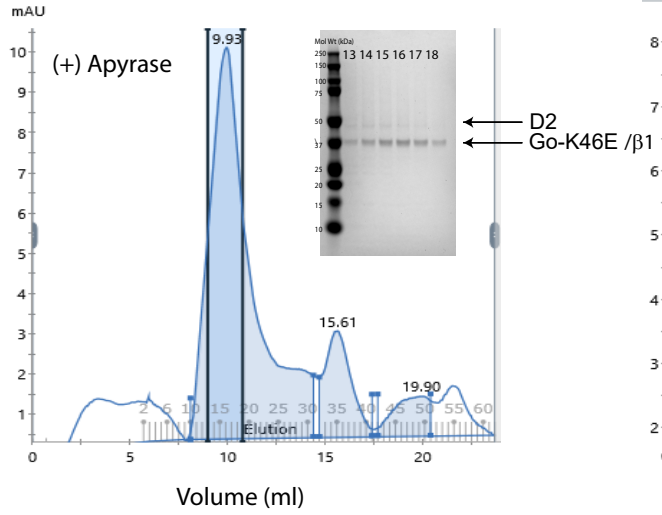

B

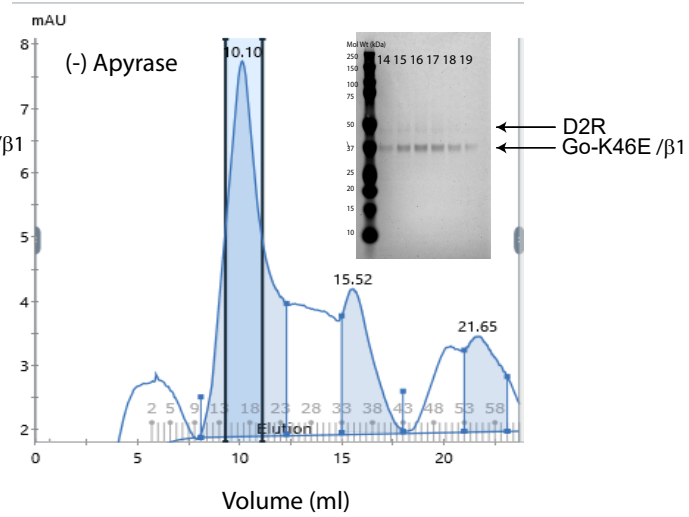

Supplementary Figure 3. Size Exclusion Chromatography (SEC) of D2R-G_o^{K46E}-$\beta_1\gamma_2$ complex +/- apyrase.

(A) SEC profile of complex purified in the presence of apyrase enzyme for the degradation of ATP/GTP to AMP/GMP.
(B) SEC profile of complex purified in the absence of apyrase enzyme representing complex formation in the presence of physiological concentrations of ATP/GTP. y-axis is displayed as absorbance units at 280 nm (mAU), x-axis is displayed as volume in milliliter (ml). Retention time is displayed above each peak. Insert is SDS gel of complex peak fractions. Molecular weight of components, D2R (50.9 kDa), G_o^{K46E} (40.0 kDa), β_1 (39.4 kDa), γ_2 (7.8 kDa) (not seen on gel).

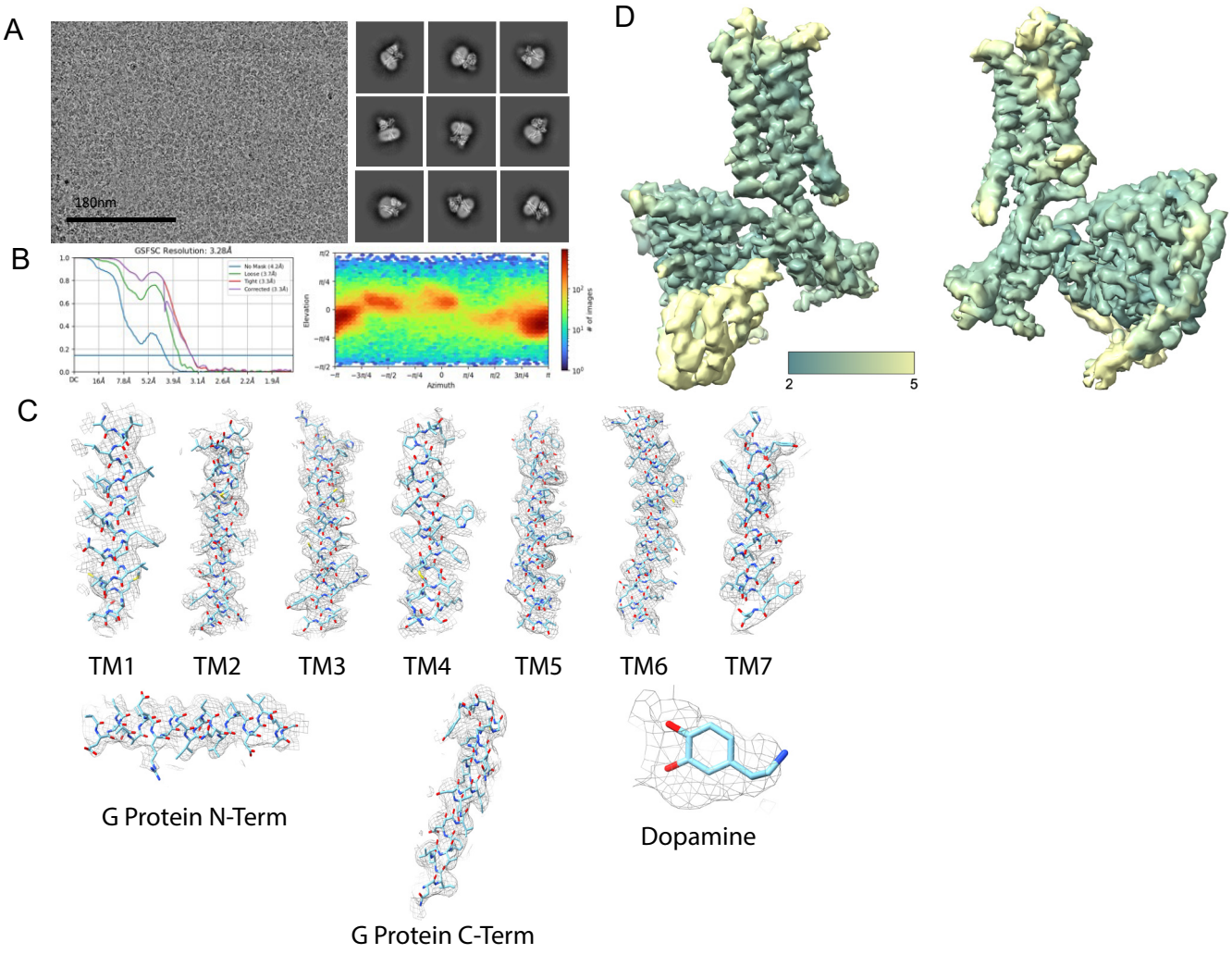

Supplementary Figure 4. Extended Cryo-EM analysis for D2R-GoK46E-β1γ2-scFv16 bound to dopamine.

(A) Select motion corrected cryo-EM micrograph of D2R-GoK46E-β1γ2-scFv16 particles imaged at a nominal magnification of 45,000 and select two-dimensional class averages.

(B) 2D plot of the gold standard Fourier shell correlation (GSFSC) and orientational distribution heat map obtained during refinement using Cryosparc.

(C) Local cryo-EM density maps of TM1-7, G protein and dopamine.

(D) Local resolution heat-map calculated using the Local Resolution Estimation within Cryosparc. Figure generated using ChimeraX.

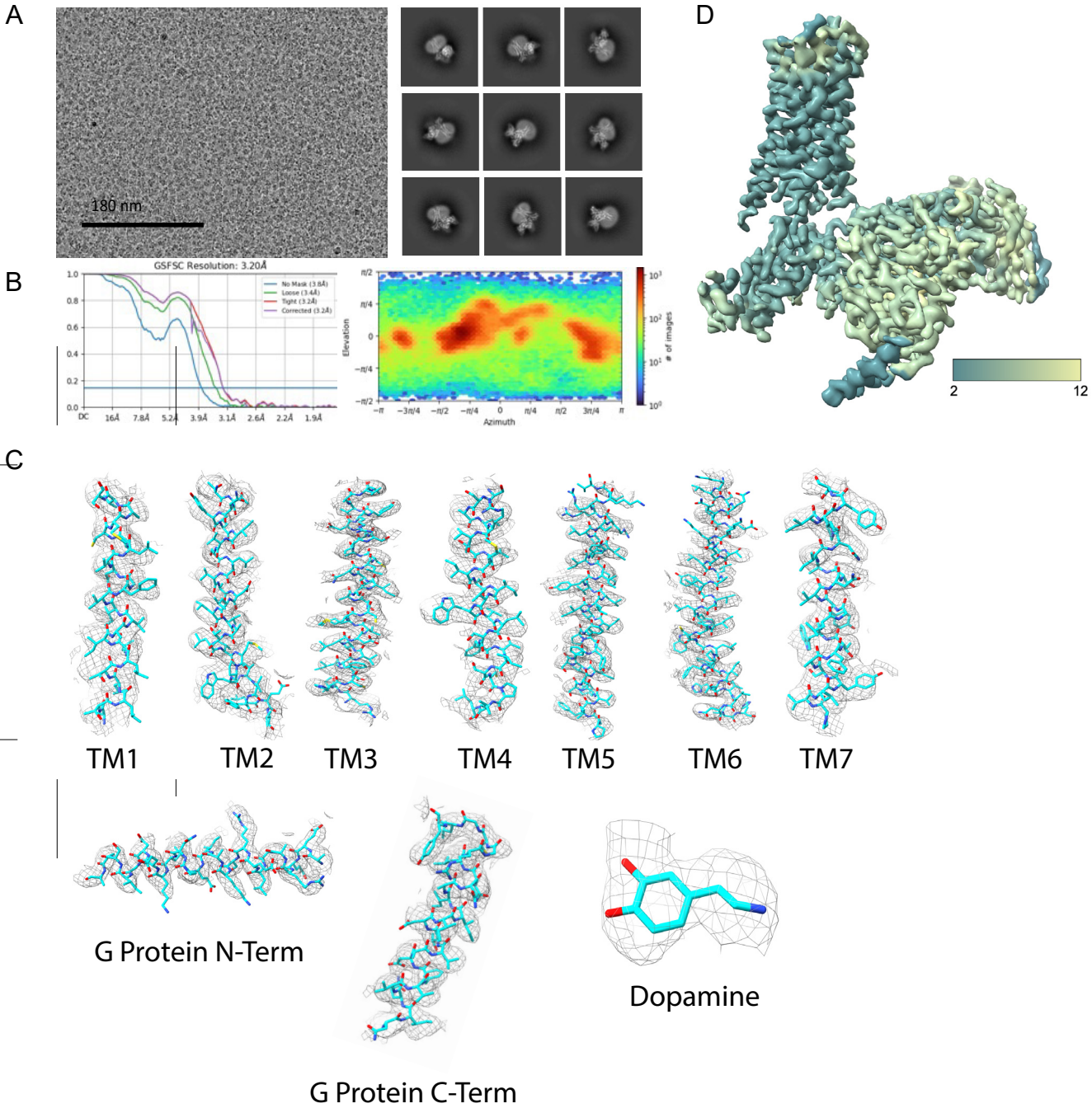

Supplementary Figure 5. Extended Cryo-EM analysis for D2R-G_o^{K46E}-$\beta_1\gamma_2$ bound to dopamine.
(A) Select motion corrected cryo-EM micrograph of D2R-G_o^{K46E}-$\beta_1\gamma_2$ particles imaged at a nominal magnification of 45,000 and select two-dimensional class averages.
(B) 2D plot of the gold standard Fourier shell correlation (GSFSC) and orientational distribution heat map obtained during refinement using Cryosparc.
(C) Local cryo-EM density maps of TM1-7, G protein and dopamine.
(D) Local resolution heat-map calculated using the Local Resolution Estimation within Cryosparc. Figure generated using ChimeraX.

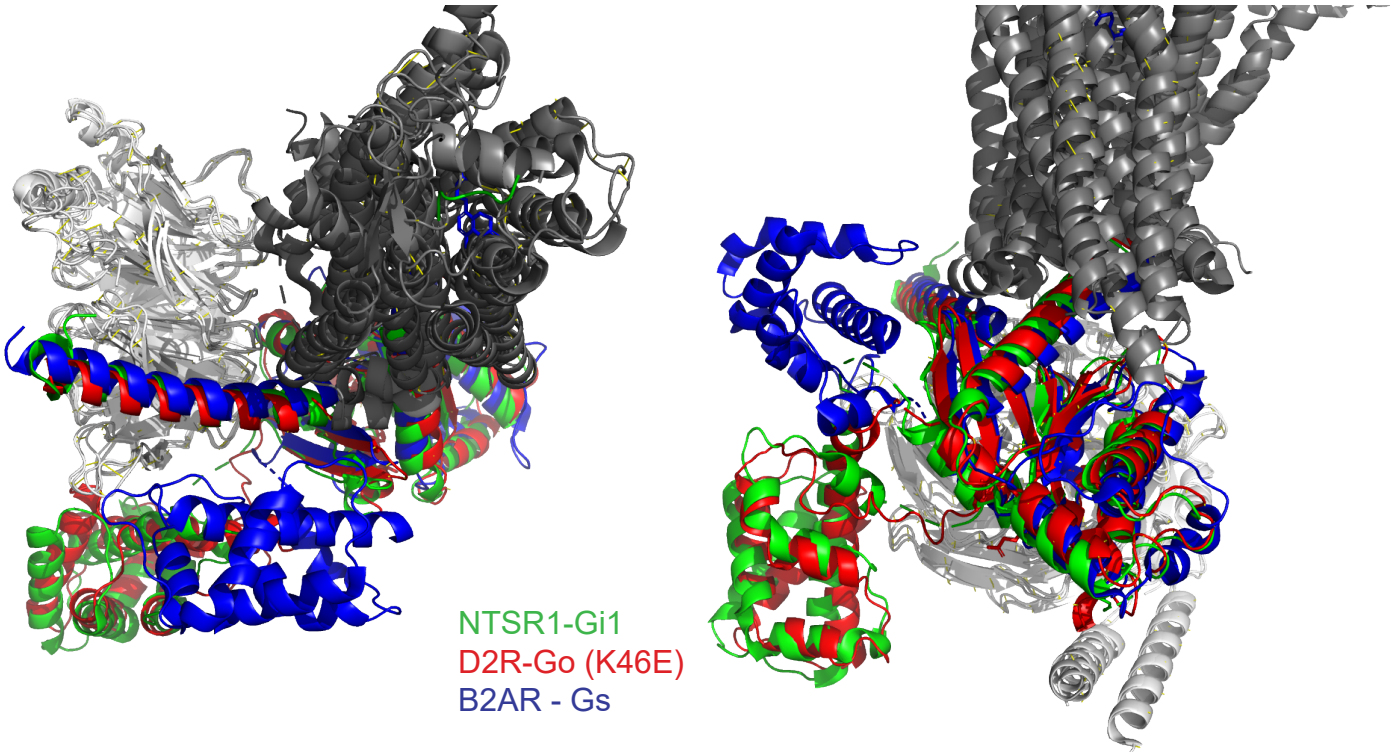

Supplementary Figure 6. Structural comparison of all-helical domains in three GPCR structures.
Overlay of NTSR1-G_{i1} (Green; PDB ID: 7L0Q[https://doi.org/10.2210/pdb7L0Q/pdb]), B2AR-G_s (Blue, PDB ID: 3SN6 [https://doi.org/10.2210/pdb3SN6/pdb]), D2R-G_o^{K46E} (Red, PDB ID: 8U02 [pending]).
GPCRs, dark grey; Gβγ, light grey.